## REMARKS

The amendment to claim 1 finds support in original claims 4 and 6, and page 5 of the specification.

Claims 1 to 6 and 12 to 15 stand rejected under 35 U.S.C. 102 (b) as being anticipated by Imamura et al. (International Journal of Hydrogen Energy, 25, 2000 pp. 837-843). However, Imamura does not disclose to use an organometallic component of the metals Zr or V as a catalyst, as now set forth in amended claim 1. The Examiner further states that it is well settled that titanium isopropoxide has a crystalline form. This is respectfully traversed. As evident from the website of Sigma Aldrich (www.sigmaaldrich.com) titanium isopropoxide is a liquid. Therefore, it cannot also have a nanocrystalline structure. Thus, claim 1 is distinguished from Imamura et al. by at least these two features.

There can be no doubt that the subject-matter of the claims is novel.

The subject-matter of the claims is also non-obvious. We enclose copy of a document (Bösenberg, et al.) which is to be published soon in "Nanotechnology". It relates to the chemical state and distribution of Zr- and V-based additives in reactive hydride composites and is authored by one of the inventors of the present application (co-authored by named inventor, R. Bormann). As evident from this reference, organometallic catalysts based on zirconium and vanadium such as zirconium isopropoxide which is exemplified in Fig. 1 on page 3 of said document have a significant influence on the desorption reaction of magnesium-containing composites such as LiBH4- MgH2. On page 2, left hand column, paragraphs 2 and 3 it is also stressed that the microstructural distribution plays an important role in the sorption kinetics. The samples were made by high-energy ball milling in a Spex 8000 mixer mill using a milling time of 5 hours. It is disclosed that the organometallic compounds therefore have a nanocrystalline structure. This is not rendered obvious by any of the documents already considered by the Examiner. All of them relate to the titanium isopropoxide or other titanium compounds as catalysts for enhancing the hydration and dehydration of hydrogen storing materials. Hence, the subject-matter of the claims is non-obvious in view of the cited prior art.

It is submitted that all claims are now of proper form and scope for allowance. Early and favorable consideration is respectfully requested.

Dated: April 16, 2009

Respectfully submitted,

By: /Richard H. Anderson Reg. #26526/

Richard H. Anderson
Registration No.: 26,526
MARSHALL, GERSTEIN & BORUN LLP
233 S. Wacker Drive, Suite 6300
Sears Tower
Chicago, Illinois 60606-6357
(312) 474-6300
Attorney for Applicants

Nanotechnology **19** (2008) 000000 (9pp) 

# On the chemical state and distribution of Zr- and V-based additives in reactive hydride composites

**U Bösenberg[1], U Vainio[2], P K Pranzas[1], J M Bellosta von Colbe[1], G Goerigk[3], E Welter[2], M Dornheim[1], A Schreyer[1] and R Bormann[1]**

[1] Institute of Materials Research, GKSS Research Centre Geesthacht, Max-Planck-Strasse 1, D-21502 Geesthacht, Germany
[2] HASYLAB at Deutsches Elektronen-Synchrotron A Research Centre of the Helmholtz Association, Notkestrasse 85, D-22607 Hamburg, Germany
[3] Institut für Festkörperforschung, Forschungszentrum Jülich, Leo-Brandt-Strasse, D-52425 Jülich, Germany

E-mail: ulrike.boesenberg@gkss.de

Received 23 June 2008, in final form 16 October 2008
Published
Online at stacks.iop.org/Nano/19/000000

*(Ed: Neil)*
Processing/NAN/
nano284535/SPE
Printed 29/10/2008
Spelling US
Issue no
Total pages
First page
Last page
File name
Date req
Artnum
Cover date

**Abstract**
Reactive hydride composites (RHCs) are very promising hydrogen storage materials for future applications due to their reduced reaction enthalpies and high gravimetric capacities. At present, the material functionality is limited by the reaction kinetics. A significant positive influence can be observed with addition of transition-metal-based additives. To understand the effect of these additives, the chemical state and changes during the reaction as well as the microstructural distribution were investigated using x-ray absorption near-edge structure (XANES) spectroscopy and anomalous small-angle x-ray scattering (ASAXS). In this work, zirconium- and vanadium-based additives were added to $2LiBH_4$–$MgH_2$ composites and $2LiH$–$MgB_2$ composites and measured in the vicinity of the corresponding absorption edge. The measurements reveal the formation of finely distributed zirconium diboride and vanadium-based nanoparticles. The potential mechanisms for the observed influence on the reaction kinetics are discussed.

## 1. Introduction

Hydrogen is one of the favored energy carriers for the future. To make mobile application possible, a reliable storage solution has to be developed. From the safety point of view, one very promising option is the chemical storage in solid-state metal compounds, metal hydrides. For application, high gravimetric storage capacities coupled with suitable desorption temperatures need to be mastered. From the thermodynamic point of view, no single, pure metal or complex hydride fulfills the requirements concerning reaction enthalpies and desorption temperature simultaneously. Alloying or the formation of intermetallic compounds is a well-known method of thermodynamic tuning since the pioneering work of Libowitz *et al* [1]. Trying to destabilize $MgH_2$, Reilly and Wiswall [2, 3] were the first, who, by adding $MgCu_2$ to $MgH_2$, discovered that reaction enthalpies can be decreased by additives which react exothermically with the hydride during desorption. These approaches are usually accompanied by a significant decrease in the gravimetric capacity of the hydride due to the combination with heavier metal elements like, for example, copper or nickel. To overcome this drawback, recently the reactive hydride composites (RHCs) were developed [4–7]. In these a chemical reaction between two or more hydrides lowers the overall reaction enthalpy while the gravimetric hydrogen storage capacity remains high. In the present work, the focus is put on the $2LiBH_4$–$MgH_2$ composites forming $2LiH$–$MgB_2$ composites in the desorbed state. This system shows a reversible hydrogen capacity of approximately 10.5 wt% and a theoretically assessed reaction enthalpy of 46 kJ $mol^{-1}$ $H_2$, leading to an estimated equilibrium temperature of 170 °C at 1 bar $H_2$. However, at

 

present the desorption occurs in a two-step reaction mechanism and takes only place at elevated temperatures with slow kinetics [8–11]. A significant improvement can be observed upon the addition of transition-metal-based additives. This is not a surprising observation, because for the well-known light metal hydrides $MgH_2$ and $NaAlH_4$ transition-metal-based additives play a crucial role in the reaction kinetics and reversibility; see e.g. [12, 13]. However, it should be noted that in the case of $NaAlH_4$ the mechanism is not yet fully understood.

So far, the description of the effect of the additives in RHCs has been mainly phenomenological in terms of the reaction kinetics. To understand the underlying mechanism, a knowledge of the chemical state and the microstructural distribution is necessary. The herein added vanadium chloride ($VCl_3$), zirconium chloride ($ZrCl_4$) and zirconium isopropoxide isopropanol (Zr-iso) are highly reactive: reactions during the high-energy ball milling process for material preparation are likely, and a change in the chemical state is therefore probable. For application, not only is the chemical state after synthesis important, but also the evolution during the cycling and the stability. In the present study, the chemical state of the zirconium-based additives has been investigated by x-ray absorption near-edge structure spectroscopy (XANES) after synthesis and after the first and the second sorption reaction. From this analysis, conclusions on the local structure around the atoms of a selected element like the valence state and the local symmetry and therefore on the bonding are drawn by comparison with reference materials.

Besides the chemical state, the microstructural distribution of the reacting phases as well as of the additive phase plays an important role in the sorption kinetics. Many common techniques such as, for example, electron microscopy cannot be applied or can be applied only with certain precautions, because the materials react readily with air. Furthermore, they are only partially stable under the electron beam, display poor conductivity and the light elements such as hydrogen, lithium and boron cannot be detected by standard techniques such as energy-dispersive x-ray spectroscopy (EDX). High resolution must be reached to characterize the fine microstructure of the nanocrystalline composites. Nevertheless, such studies are possible, and first transmission electron microscopy (TEM) investigations on the currently investigated RHCs with titanium-based additives display a uniform distribution of titanium in the sample down to an observed size scale of approximately 200 nm [14]. This indicates a very fine additive distribution and sizes much smaller than 200 nm for the corresponding additive phase. But high or atomic resolution has not yet been achieved for these compounds and therefore information on the local structure and chemical state was not obtained.

To characterize the nanostructure of a material, small-angle scattering (SAS) using neutrons (SANS) or photons (SAXS) is a well-known tool, giving also the advantage of averaging over the whole sample rather than probing locally. The intensity of the scattered radiation at angles below 5° is recorded to analyze structures in the range of typically 0.5–100 nm and can be applied for samples with different structure, such as solid, liquid or amorphous. In anomalous small-angle x-ray scattering (ASAXS) the change in the complex scattering factors at the absorption edge of the respective element leads to a change in the scattered intensity as a function of energy. By measuring at several energies in the vicinity of the absorption edge, the scattering contribution from the respective element (i.e. V or Zr) contained in the structures can be separated from the total scattering coming from the material [15]. The absorption edges of metallic Zr and V are at 17 998 eV and 5465 eV, respectively.

The present study gives the first insight into the chemical state and distribution of V- and Zr-based additives in reactive hydride composites and contributes to the understanding of the mechanism by which transition-metal-based additives influence the sorption kinetics.

## 2. Experimental details

### *2.1. Sample preparation*

All samples were prepared by high-energy ball milling in a Spex 8000 mixer mill, using a ball to powder ratio of 10:1 and a milling time of 5 h. The initial microcrystalline powders, $LiBH_4$ (95% purity), LiH (99.4% purity), $MgB_2$, $VCl_3$, $ZrCl_4$ and Zr isopropoxide isopropanol complex (Zr-iso) were purchased from Alfa Aesar. $MgH_2$ (98% purity, the rest being Mg) was obtained from Goldschmidt. 10 mol% additive was added to the initial mixture of $2LiH + MgB_2$. For the initial $2LiBH_4$–$MgH_2$ composites, the $MgH_2$ was pre-milled for 5 h before the $LiBH_4$ and 10 mol% additive were added. The comparatively large amount of additive ensured a good contrast during the measurements.

To obtain the different sorption states, cycling was performed in a Sievert's type apparatus, designed by HERA Hydrogen Systems, Hydro Quebec, employing 5 bar hydrogen back pressure for the desorption reaction at a constant temperature of 400 °C. Absorption was performed under 30 or 50 bar hydrogen at 350 °C. The same materials were used for the ASAXS and the XANES measurements with approximately four weeks between the experiments.

All preparation and handling of the materials was performed in continuously purified argon atmosphere in a glovebox.

### *2.2. X-ray absorption near-edge structure (XANES)*

XANES measurements have only been performed on the Zr-containing samples so far. The samples were mixed with cellulose and pressed into pellets of 11 mm in diameter. These pellets were mounted between two 55 $\mu$m Kapton tapes on aluminum sample holders. The samples were then measured three times for approximately one hour in the energy range 17 200–19 000 eV under vacuum conditions at beamline A1, Hasylab, DESY [16, 17].

### *2.3. Anomalous small-angle x-ray scattering (ASAXS)*

For ASAXS measurements, the Zr-containing powders were put in 1 mm thick sample holders of aluminum with a hole of

5 mm in diameter and sealed by two 55 $\mu$m thick Kapton tapes in an argon-filled glovebox. To reach similar transmission values, the thickness for the V-containing samples had to be reduced to approximately 50 $\mu$m. The measurements were performed under vacuum conditions at beamline B1, Hasylab, DESY [18, 19]. Prior to each ASAXS measurement, a low-resolution XANES scan was measured to determine the position of the absorption edge of each sample. For the Zr-containing samples, the energy of radiation was tuned across the K absorption edge of Zr at 17 998 eV in steps of 1 eV, and similarly for the V-containing samples around 5465 eV. The flux of the direct beam and that of the beam transmitted by the sample were measured with a photodiode. The ASAXS intensities were measured at five or six energies below the previously determined absorption edges for the Zr-containing materials and at three energies for the V-containing samples. The sample-to-detector distances were 935 and 3635 mm. $q$ is defined as the magnitude of the scattering vector with $q = 4\pi \sin\theta/\lambda$, where $2\theta$ is the scattering angle and $\lambda$ the wavelength. The reliable $q$-range of the instrument in the energy range of Zr was concluded to be from 0.2 to 14 nm$^{-1}$ and in the energy range of V from 0.1 to 4 nm$^{-1}$. Three measurement cycles were performed for each sample at each energy and distance. The measured 2D data were corrected for dark current, detector response, transmission of the sample, and for geometrical distortion and integrated azimuthally. Further, the intensity was put on an absolute intensity scale by using pre-calibrated glassy carbon standards. A $q^{-4}$-dependence was fitted to the scattering data at high $q$-values and the determined constant was then subtracted to correct the data for an energy-dependent background due to resonant Raman scattering and fluorescence.

Due to the large electron density contrast between zirconium or vanadium and the hydride matrix the materials are treated as two-phase systems. The x-ray scattering intensity $I(q)$ can then be written as [20]

$$I(q, E) = x_\alpha |f_\alpha(q, E)|^2 S_{\alpha\alpha}(q) + 2x_\beta \Re[f_\alpha(q, E) f_\beta(q, E)] S_{\alpha\beta}(q) + x_\beta |f_\beta(q, E)|^2 S_{\beta\beta}(q) \quad (1)$$

where $f(q, E) = f_0 + f'(q, E) + \mathrm{i}f''(q, E)$ is the atomic scattering factor, where $f_0 = Z$, the number of electrons (atomic number) and $f'(q, E)$, $f''(q, E)$ are the so-called anomalous dispersion corrections. The dependence of $f$ on $q$ is small for small angles and is here neglected. $x_\alpha$ and $x_\beta$ correspond to the atomic fractions of the two phases $\alpha$ and $\beta$, and the $S$ are the partial structure factors (PSFs). Only the real part $\Re$ of the cross term contributes to the scattering intensity because the imaginary parts cancel each other out for $S_{12} = S_{21}$. The PSF for zirconium $S_{\beta\beta}$ could not be solved reliably from equation (1), nor by using the derivative method described in [21], because no stable solution could be obtained. However, the scattering contribution from the cross term $S_{\alpha\beta}(q)$ was assessed to be small within the resolved $q$-range and it was therefore neglected for the further analysis. Then the difference between two intensities measured at two energies gives the PSF for zirconium. The change in $f'$ between the two energies was about 5.3. The anomalous dispersion corrections, $f'$ and $f''$, were obtained from the XANES measurements using the CHOOCH program [22, 23], and are tabulated with the corresponding energies in table 1. The edge position for each sample was determined experimentally from the XANES measurements at beamline A1 by determination of the first inflection point of the derivative as described in [24].

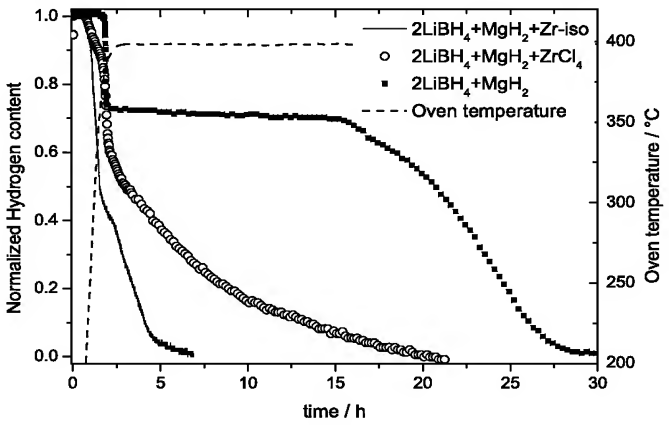


**Figure 1.** Volumetric measurements of the first desorption reaction of $2LiBH_4$–$MgH_2$ composites with 10 mol% $ZrCl_4$ or Zr-iso compared to the material without additives.

To analyze the size distribution of the Zr-containing compounds, the Debye–Bueche model was used. It is a simple two-phase model with sharp interfaces but random shape and distribution of the phase. Debye [25] first developed and applied the model, and recently it was applied by Goerigk and Williamson [26, 27] on ASAXS data. The separated scattering curves were fitted by the following model function:

$$I(q) = \frac{ba^3}{(1 + a^2q^2)^2} + \frac{c}{q^4} \quad (2)$$

with the correlation length $a$, from which the two correlation lengths of the phases $\alpha$ and $\beta$, $\xi_\alpha$ and $\xi_\beta$, are calculated according to $1/a = 1/\xi_\alpha + 1/\xi_\beta$ and $\xi_\beta = a/(1 - \Phi_\beta)$. $\Phi_\beta$ corresponds to the volume fraction of the Zr-containing phase $\beta$. Constant $b$ includes information on the volume fraction, density and concentration of phase $\beta$. However, the equations described in [27] cannot be solved for $b$ in this case, because the density of the material and, due to the ongoing chemical reactions, exact composition are not known. Therefore the volume fractions were estimated from the chemical formula of the composites. The additional $c/q^4$-term takes large Zr-containing inhomogeneities into account; $c$ is a constant.

## 3. Results

In figure 1 the kinetic behavior of the desorption reactions, obtained by volumetric measurements, is shown. As Zr is a heavy element, and due to possible reactions, the storage capacities are drastically reduced to approximately 5.5 wt% in the case of the samples with 10 mol% Zr-iso- and 7.5 wt% for the 10 mol% $ZrCl_4$-containing samples. For better comparison, the reactions are normalized in the graphic. The materials were

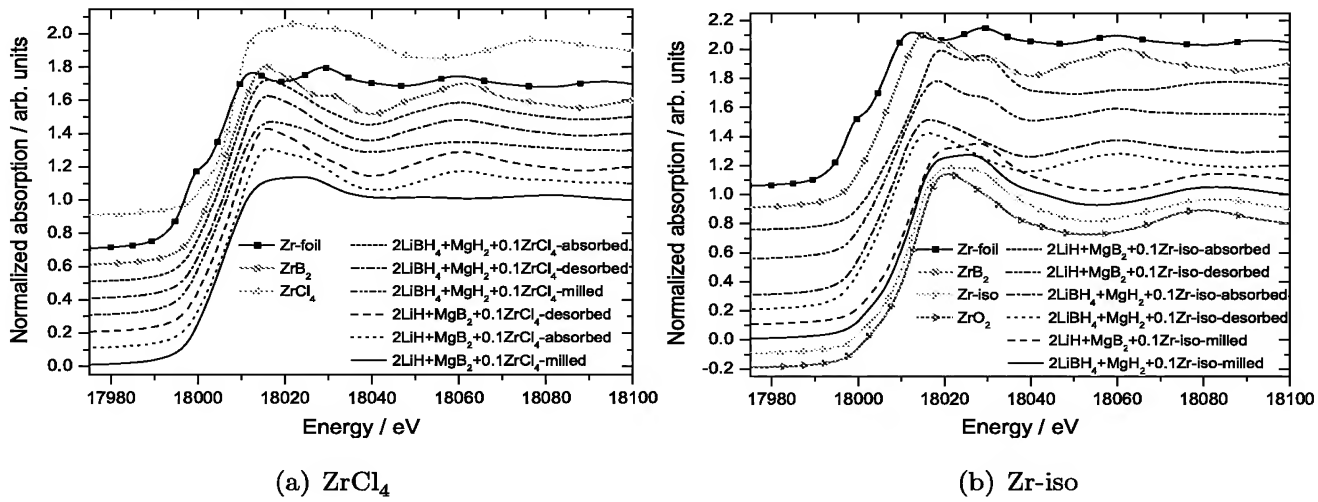


**Figure 2.** XANES curves of the samples with the respective additives. The curves are shifted vertically for better visualization.

**Table 1.** Anomalous dispersion corrections obtained from the XANES measurements at beamline A1 for each applied energy and the experimentally determined absorption edge position for each sample.

| Sample | ASAXS energies (eV) | $f'$ | $f''$ | Edge energy (eV) |
|---|---|---|---|---|
| $2LiBH_4 + MgH_2 + 0.1ZrCl_4$-milled | 17 645 | −3.05 | 0.56 | 18 007 |
| | 18 003 | −7.63 | 1.91 | |
| $2LiBH_4 + MgH_2 + 0.1ZrCl_4$-desorbed | 17 645 | −3.05 | 0.56 | 18 008 |
| | 18 006 | −7.78 | 2.5 | |
| $2LiBH_4 + MgH_2 + 0.1ZrCl_4$-absorbed | 17 645 | −3.05 | 0.56 | 18 008 |
| | 18 006 | −7.84 | 2.47 | |
| $2LiBH_4 + MgH_2 + 0.1$Zr-iso-milled | 17 641 | −3.02 | 0.56 | 18 012 |
| | 18 001 | −7.05 | 1.02 | |
| $2LiBH_4 + MgH_2 + 0.1$Zr-iso-desorbed | 17 641 | −3.04 | 0.56 | 18 009 |
| | 18 001 | −7.51 | 1.48 | |
| $2LiBH_4 + MgH_2 + 0.1$Zr-iso-absorbed | 17 641 | −3.04 | 0.56 | 18 009 |
| | 18 001 | −7.51 | 1.46 | |
| $2LiH + MgB_2 + 0.1ZrCl_4$-milled | 17 648 | −3.03 | 0.54 | 18 006 |
| | 18 003 | −7.25 | 1.8 | |
| $2LiH + MgB_2 + 0.1ZrCl_4$-desorbed | 17 645 | −3.02 | 0.54 | 18 009 |
| | 18 006 | −7.65 | 2.32 | |
| $2LiH + MgB_2 + 0.1ZrCl_4$-absorbed | 17 645 | −3.02 | 0.54 | 18 009 |
| | 18 006 | −7.63 | 2.22 | |
| $2LiH + MgB_2 + 0.1$ Zr-iso-milled | 17 641 | −2.99 | 0.51 | 18 013 |
| | 18 001 | −6.29 | 0.96 | |
| $2LiH + MgB_2 + 0.1$ Zr-iso-desorbed | 17641 | −3.04 | 0.56 | 18 009 |
| | 18 001 | −7.36 | 1.29 | |
| $2LiH + MgB_2 + 0.1$ Zr-iso-absorbed | 17645 | −3.05 | 0.56 | 18 007 |
| | 18 006 | −7.76 | 2.48 | 18014 |
| Zr-powder | | | | 17 998 |
| $ZrB_2$ | | | | 18 008 |
| $ZrCl_4$ | | | | 18 009 |
| Zr-iso | | | | 18 012 |

measured under a back pressure of 5 bar $H_2$ and isothermal conditions of 400 °C. Under these conditions a two-step reaction is observed. The pure composite suffers from severe kinetic constraints with a lengthy incubation period between the two desorption steps. The impact of the additives especially on the incubation period is significant. Furthermore, there is also an impact on the reaction rates for the second step of the reaction, where Zr-iso reveals the highest reaction rates. In case of the $ZrCl_4$-containing sample, the reaction rate for the second step decelerates during desorption. This beneficial effect of the additives is sustainable also for further sorption reactions leading to similar kinetics. The possible origin of the effect will be discussed below.

XANES data of the reference samples, and milled and cycled samples are shown in figure 2. For these data, the initial intensities from the three measurement cycles were added, the sloped background before the edge subtracted and then they were normalized to the value at 18 100 eV. As reference

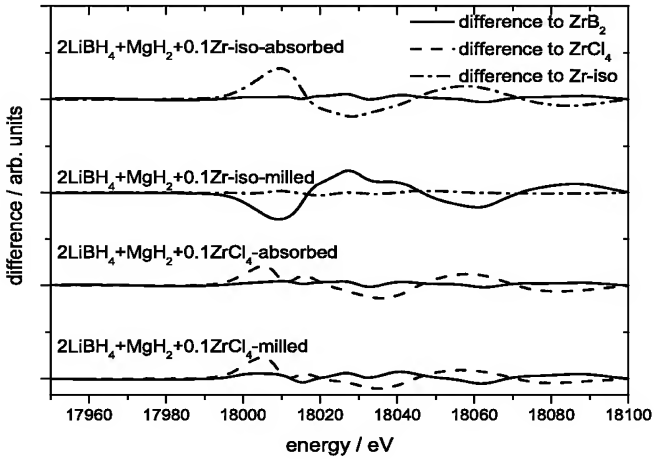


**Figure 3.** Difference curves of the XANES measurements for four selected samples to $ZrCB_2$, Zr-iso or $ZrCl_4$.

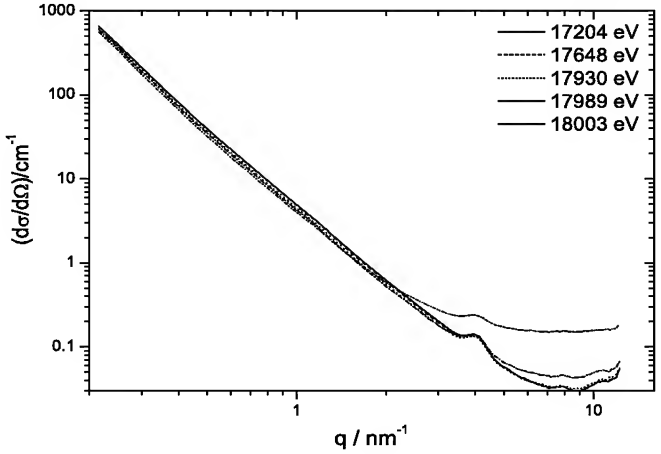


**Figure 4.** SAXS data for the sample $2LiBH_4 + MgH_2 + 0.1ZrCl_4$-milled obtained at 17 200, 17 648, 17 930, 17 989 and 18 003 eV.

materials Zr metal, $ZrO_2$, $ZrB_2$ and the initial additives Zr isopropoxide isopropanol (Zr-iso) and $ZrCl_4$ were measured.

The curves obtained for the materials prepared with additional $ZrCl_4$ show little similarity to the initial absorption edge of $ZrCl_4$. In these samples the position of the edge was the same; see table 1 for comparison. There are some variations in the amplitude of the oscillations in the post-edge region. They are probably due to the nanocrystalline state of the compound. The materials are apparently reduced during the milling, however not to metallic Zr, because the absorption edge is slightly shifted to lower energies but not to the value of metallic Zr. The state is stable upon further cycling. For these samples, the formation of $ZrB_2$ is proposed. This is illustrated in figure 3 by the difference curves of milled and cycled $2LiBH_4 + MgH_2 + 0.1ZrCl_4$ composites to $ZrCl_4$ and $ZrB_2$. The XANES results of all $ZrCl_4$-containing samples show a very high similarity to those obtained for pure $ZrB_2$ and significant differences to the initial $ZrCl_4$.

The matter is more difficult for the materials prepared with additional Zr-iso. Upon milling, there seem to be no changes in the chemical state, which is also confirmed by the Bragg peaks of Zr-iso measured in the ASAXS measurements and the similarity to the initial Zr-iso in figure 3 of the $2LiBH_4 + MgH_2 + 0.1Zr$-iso composites. After the first sorption reaction, the Zr is reduced to a lower valency state, indicated by a shift of the absorption edge to lower energy; see table 1. Also the bonding has changed, as indicated by the post-edge peak positions. For example, in the region of 18 060 eV, the milled samples display a minimum, whereas after the first cycle a maximum is displayed. Investigations by other methods such as *in situ* x-ray diffraction as well as differential scanning calorimetry indicate a reaction with the composite around 300 °C during the first heating. The formation of a $ZrB_2$ phase then is likely. $ZrB_2$ is observed for the cycled samples of initial $2LiBH_4 + MgH_2 + 0.1Zr$-iso composites; in figure 3 the difference curve to $ZrB_2$ is almost zero. In the first sorption reactions in $2LiH + MgB_2 + 0.1Zr$-iso composites, the Zr is slightly reduced but the edge position has not reached the typical edge position for $ZrB_2$. A stable state is not reached and a mixture of different chemical states of Zr is likely after one sorption cycle for these composites. The details of the chemical state of the additives such as Zr- as well as Ti- and V-based additives by x-ray absorption spectroscopy are the subject of further study.

In figure 4, the original scattering curves for all energies are shown exemplarily for the sample $2LiBH_4 + MgH_2 + 0.1ZrCl_4$-milled. The shift of the intensity to lower values with increasing energy is significant. The broad peak at approximately 4 $nm^{-1}$ is caused by the Kapton tape of the sample holder. The high scattering cross section at high $q$-values for the measurements at the higher energies are due to resonant Raman scattering and fluorescence. This constant background was subtracted prior to further analysis.

The obtained separated curves from the ASAXS measurements are shown for all samples in figure 5, where the symbols present the experimental data and the lines the fits according to equation (2). The fitted correlation lengths are listed in table 2. In combination with the estimated volume fraction for $ZrB_2$, the characteristic length of the $ZrB_2$ ($\xi_\beta$) and of the hydride matrix ($\xi_\alpha$) are calculated. However, the value of the volume fraction is not known exactly, as the chemical state is assumed to be homogeneous in the sample and the density of the bulk materials is considered and the porosity neglected in the calculations. Therefore the matrix length $\xi_\alpha$ can only serve as an estimate. However, it matches nicely the estimated crystallite sizes.

The milled composites with additional Zr-iso reveal no structures in the measured size range of approximately 0.4 to 30 nm and show only scattering from larger structures. The peak at 7 $nm^{-1}$ is a Bragg peak attributed to the Zr-iso in the milled composite. The lack of small structures is therefore reasonable. Upon cycling, distinct changes become noticeable. For the materials with additional Zr-iso a hump at approximately 2 $nm^{-1}$ forms and becomes more pronounced with cycling. This corresponds to structures with a size of around 1 nm. These observations cannot be translated

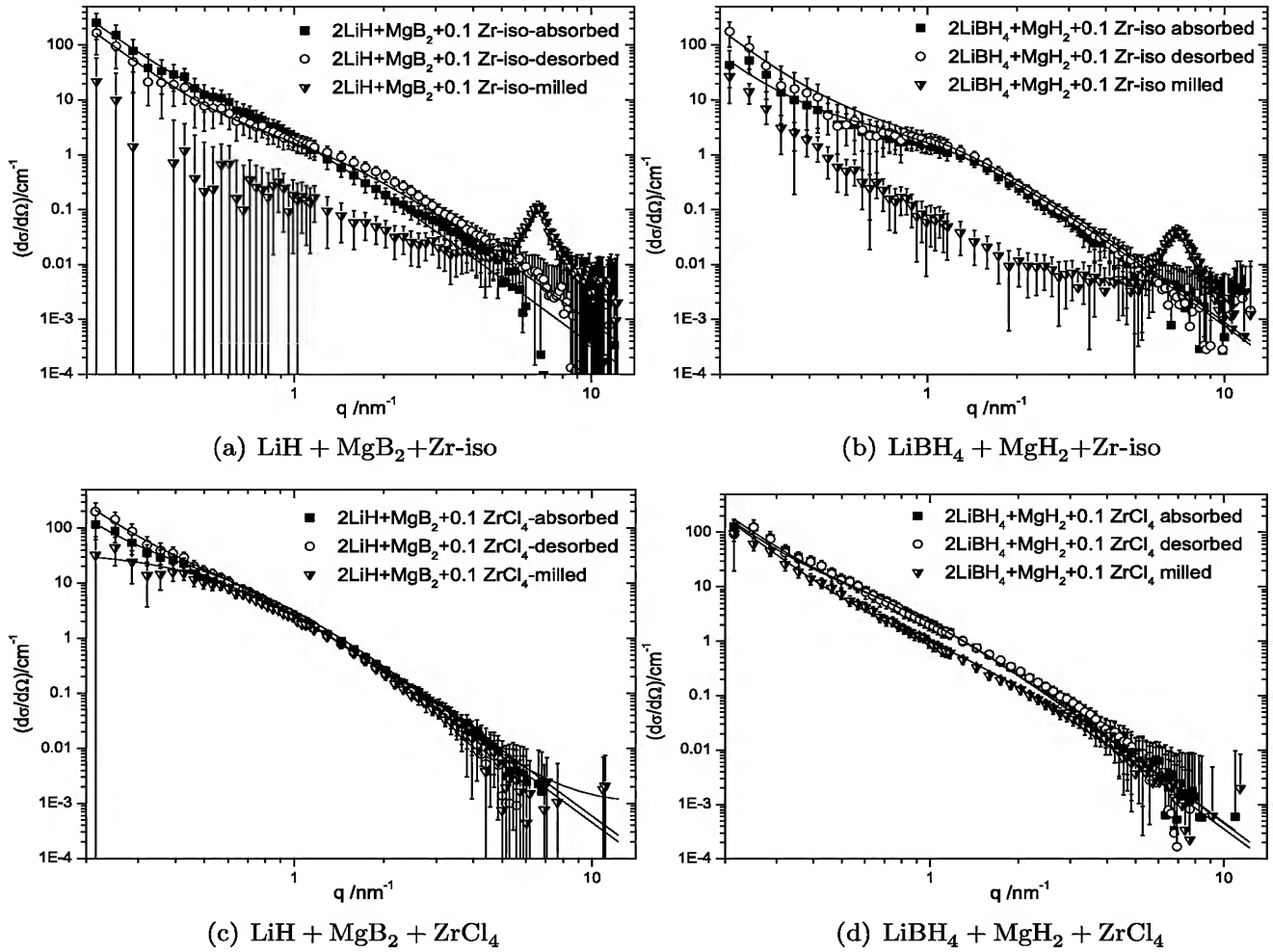


**Figure 5.** Separated scattering curves for the as-prepared and cycled composites obtained from ASAXS measurements at the K absorption edge of Zr at 17 998 eV. The symbols represent the measured data whereas the lines correspond to the obtained fit applying the Debye–Bueche model described by equation (2).

directly to materials with additional $ZrCl_4$. In the latter case stable $ZrB_2$ nanoparticles seem to have formed during milling. The associated correlation lengths are approximately 1–2 nm. They remain almost constant upon further cycling. For the LiH–$MgB_2$ composites with additional $ZrCl_4$, an additional formation of larger inhomogeneities can be observed due to the increased scattering in the small $q$-region.

Due to poor detector sensitivity at the low energies in the case of the V-containing samples (5465 eV), only the scattering results from the sample set of $2LiH + MgB_2 + 0.1VCl_3$ could be reliably analyzed. For these samples, very similar results were obtained. The results for $2LiH + MgB_2 + 0.1VCl_3$ composites in different cycling states are shown in figure 6.

The fitting results reveal similar characteristic lengths of 1 to 2.5 nm for V-based additives. Besides the fitting, the slope of the scattering cross section contains information on the shape of the structures. Proportionalities to $q^{-3}$ and $q^{-2.5}$ were estimated for composites with Zr-based additives and V-based additives, respectively. This is an indication for mass fractals or polydispersity and especially for the V compounds a formation of slightly anisotropic structures is likely.

In figure 7, the separated scattering curves for the sample $2LiBH_4 + MgH_2 + 0.1$Zr-iso-absorbed and the distance distribution function fitted using the GNOM program [28] is shown. The distance distribution shows the probability of distances between scattering centers in the sample and gives an estimate of the maximum sizes that are present in the sample. Figure 7(b) shows exemplarily the width of the distance distribution of the Zr-containing structures with maximum length of about 4 nm and a maximum around 2 nm, which is in good agreement with the previously determined correlation length; see table 2. For this fit, the scattering from larger inhomogeneities at low $q$-values was neglected. Similar distance distributions were obtained for all samples.

## 4. Discussion

The results obtained in this study show that in all the investigated cases the transition-metal-based additives ($VCl_3$, $ZrCl_4$, Zr-iso) show a very fine distribution, either already after milling or after the first sorption reactions. For the

**Table 2.** Characteristic length obtained by fitting with the Debye–Bueche model.

| Sample | Correlation length $a$ (nm) | Volume fraction $\Phi_\beta$ | $\xi_\beta$ (nm) | $\xi_\alpha$ (nm) |
|---|---|---|---|---|
| $2LiBH_4 + MgH_2 + 0.1ZrCl_4$-absorbed | 1.4 | 0.023 | 1.4 | 60.9 |
| $2LiBH_4 + MgH_2 + 0.1ZrCl_4$-desorbed | 1.4 | 0.04 | 1.4 | 35.0 |
| $2LiBH_4 + MgH_2 + 0.1ZrCl_4$-milled | 0.9 | 0.023 | 0.9 | 39.1 |
| $2LiBH_4 + MgH_2 + 0.1$Zr-iso-absorbed | 0.9 | 0.03 | 0.9 | 30.0 |
| $2LiBH_4 + MgH_2 + 0.1$Zr-iso-desorbed | 0.9 | 0.03 | 0.9 | 30.0 |
| $2LiH + MgB_2 + 0.1ZrCl_4$-absorbed | 1.6 | 0.023 | 1.6 | 69.6 |
| $2LiH + MgB_2 + 0.1ZrCl_4$-desorbed | 1.7 | 0.04 | 1.8 | 42.5 |
| $2LiH + MgB_2 + 0.1ZrCl_4$-milled | 1.8 | 0.04 | 1.9 | 45.0 |
| $2LiH + MgB_2 + 0.1$Zr-iso-absorbed | 1.5 | 0.03 | 1.5 | 50.0 |
| $2LiH + MgB_2 + 0.1$Zr-iso-desorbed | 0.8 | 0.03 | 0.8 | 26.7 |
| $2LiH + MgB_2 + 0.1VCl_3$-absorbed | 2.0 | 0.03 | 2.1 | 40.0 |
| $2LiH + MgB_2 + 0.1VCl_3$-desorbed | 2.4 | 0.03 | 2.5 | 60.0 |
| $2LiH + MgB_2 + 0.1VCl_3$-milled | 2.0 | 0.03 | 2.1 | 40.0 |

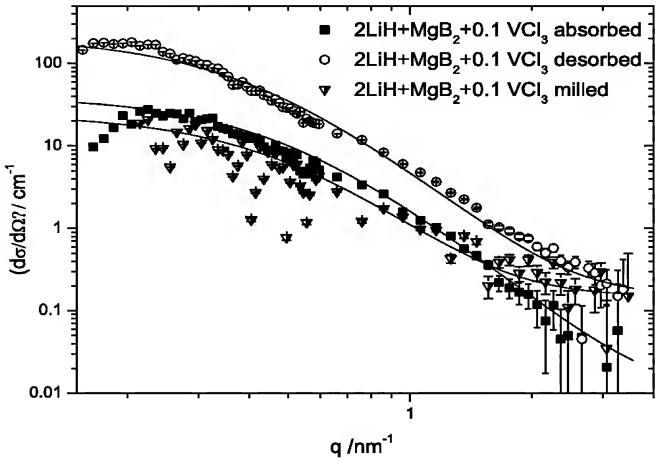


**Figure 6.** Separated scattering curves for $2LiH + MgB_2 + 0.1\ VCl_3$ composites in the milled, absorbed and desorbed state obtained from ASAXS measurements at the K absorption edge of V at 5465 eV.

Zr-based additives, the formation of stable $ZrB_2$ is proposed; for V-based additives a similar XANES study is currently being performed. An average precipitation size of the transition metal compounds of 1–2 nm was determined by fitting a correlation length model.

In comparison with the literature for $TiB_2$ precipitations in $MgB_2$ by doping with Ti, a distribution of very fine nanoparticles in the grain boundaries as well as in the matrix was observed by TEM investigations [29, 30]. A segregation of the precipitates in the grain boundaries may be reasonable, because the sorption reactions involve complex phase transformation with significant mass transport. The precipitates could be swept into the grain boundaries and prevent coarsening by stabilization of the grain boundaries. This is supported by the fact that from the crystallite sizes, assessed for the Mg phases by applying the Scherrer equation, no significant coarsening can be observed after the sorption processes (data not shown). A formation of a network of the Zr- or V-based compounds in the grain boundaries could also lead to the observed scattering from larger structures observed at low $q$-values. In all cases with Zr- or V-based additives, a significant enhancement of the reaction kinetics could be observed in volumetric measurements. In particular, the reduction of the incubation period between the two desorption steps is striking. In an earlier study, a nucleation problem of $MgB_2$ was proposed to be the origin of the incubation period. Calculations have shown that the lattice misfits, which are important factors for heterogeneous nucleation, are rather small for $MgB_2$ on $ZrB_2$ or $VB_2$ because the three phases have the same hexagonal lattice structure. Therefore the observed $ZrB_2$ might act as a nucleation agent for $MgB_2$. Furthermore, borides, especially $TiB_2$, are known as outstanding grain refiners in Mg alloys and Al alloys [31, 32]. Recently, *in situ* neutron diffraction study by Singh *et al* [33] on $NaAlH_4$ supports the correlation of small grains and sites for heterogeneous nucleation with the catalyst. They have observed a significant grain coarsening for uncatalyzed $NaAlH_4$ while for the samples with $TiCl_3$-catalyzed $NaAlH_4$ the grain size remained small during the sorption reactions.

However, the different reaction rates obtained for the two additives $ZrCl_4$ and Zr-iso indicate that this is probably not the only explanation. Already in a simple binary light weight hydride system like $MgH_2$, the function of transition metal compound additives and especially transition metal oxides is rather complex. According to Dornheim *et al* [34], transition metal oxides do not only accelerate the surface reaction kinetics by a catalytic effect but also have a clear influence on the $MgH_2$ particle size during milling as well as the stabilization of crystallite sizes during cycling at elevated temperatures. Zhou [35] modeled the kinetics of LiH–$MgB_2$ composites with different transition metal additives based on a series of volumetric measurements. According to the different shapes of the respective absorption and desorption curves, they concluded that the use of different additives leads to different rate-limiting steps for the reactions of the RHC. This indicates that the effect of the additives on the reaction mechanism in the composites is rather complex and that there will be no single explanation for the different additives and their effect on the reaction kinetics.

In the literature no study was found which would support a potential catalytic activity of the $ZrB_2$ for hydrogen splitting or recombination. For example, early measurements by Lavrenko *et al* [36] and Samsonov and Kharmalov [37] revealed a rather Q.1

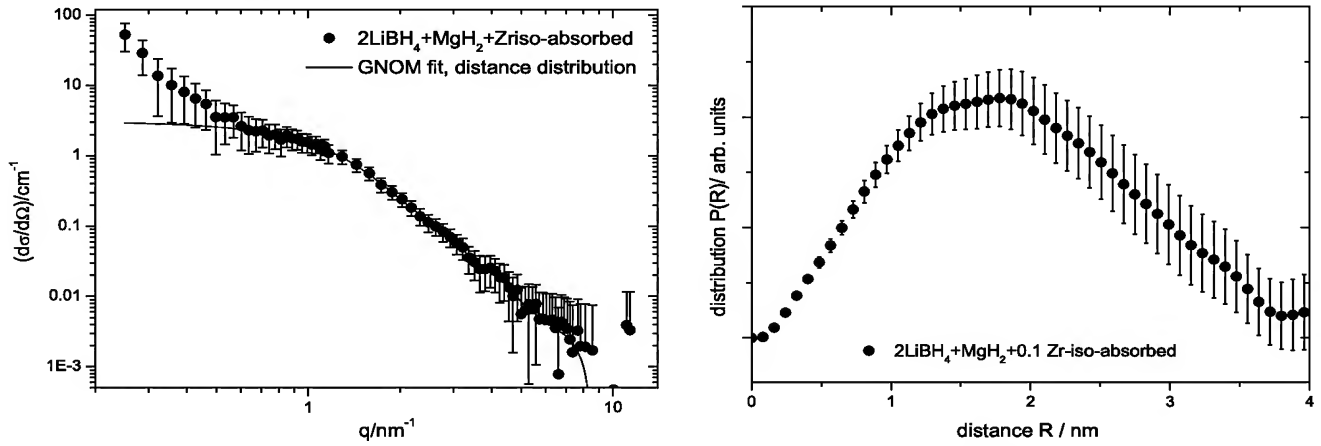


(a) Separated scattering curve (b) obtained distance distribution

**Figure 7.** Separated scattering curve for $2LiBH_4 + MgH_2 + 0.1Zr$-iso-absorbed composites obtained from ASAXS measurements at the K absorption edge of Zr at 17 998 eV and the corresponding distance distribution using the GNOM program.

low activity of $ZrB_2$ with respect to hydrogen. This is related to the charge-free surfaces. In any case, a catalytic effect of $ZrB_2$ on the hydrogen reaction should lead to similar sorption rates since $ZrB_2$ is formed in both investigated cases, and the size and distribution are similar.

As indicated by this discussion, numerous origins for the reaction enhancement with additional transition metal additives are possible. A combination of multiple effects may therefore also be likely.

## 5. Conclusions

Transition-metal-based additives have a significant influence on the sorption kinetics of reactive hydride composites such as $2LiBH_4$–$MgH_2$ composites. In the present study, the chemical state and the microstructural distribution of the Zr- and V-based additives, $ZrCl_4$, Zr isopropoxide isopropanol complex and $VCl_3$ were investigated by means of XANES and ASAXS. For the first time the chemical state and distribution of the transition metal compound formed by these additives for reactive hydride composites has been experimentally determined by the use of XANES/ASAXS. The formation of $ZrB_2$ or V-based nanoparticles with a typical length scale of 1–2 nm is proposed for Zr- or V-based additives. How these nanoparticles influence the reaction kinetics in detail remains unclear and is the subject of further studies.

## Acknowledgments

Partial funding by the Helmholtz Initiative 'Functional Materials for Mobile Hydrogen Storage' is gratefully acknowledged by the authors.

## References

[1] Libowitz G, Hayes H and Gibb T 1958 *J. Phys. Chem.* **62** 76
[2] Reilly J and Wiswall R 1967 *Inorg. Chem.* **6** 2220–3
[3] Reilly J J and Wiswall R H 1968 *Inorg. Chem.* **7** 2254–6
[4] Barkhordarian G, Klassen T and Bormann R 2004 *Patent Pending, German Pub. No* 102004/061286
[5] Barkhordarian G, Klassen T, Dornheim M and Bormann R 2007 *J. Alloys Compounds* **440** L18–21
[6] Vajo J J, Mertens F, Skeith S and Balogh M 2004 *Patent Pending, Int. Pub. No* 2005/097671 A2
[7] Vajo J J, Skeith S L and Mertens F 2005 *J. Phys. Chem.* B **109** 3719–22
[8] Bösenberg U *et al* 2007 *Acta Mater.* **55** 3951–8
[9] Nakagawa T, Ichikawa T, Hanada N, Kojima Y and Fujii H 2007 *J. Alloys Compounds* **446/447** 306–9
[10] Vajo J J, Mertens F, Ahn C C, Bowman R C and Fultz B 2004 *J. Phys. Chem.* B **108** 13977–83
[11] Pinkerton F E, Meyer M S, Meisner G P, Balogh M P and Vajo J J 2007 *J. Phys. Chem.* C **111** 12881–5 Q.2
[12] Bogdanovic B and Schwickardi M 1997 *J. Alloys Compounds* **253/254** 1–9
[13] Oelerich W, Klassen T and Bormann R 2001 *J. Alloys Compounds* **315** 237–42
[14] Deprez E 2008 *Master's Thesis* University of Sevilla
[15] Stuhrmann H, Goerigk G and Munk B 1991 *Handbook on Synchrotron Radiation* (Amsterdam: Elsevier Science) chapter 17 (Anomalous X-ray Scattering) pp 555–80
[16] Attenkofer K 2000 Die magnetische Kopplung in ausgewählten Verbindungen—Neue Möglichkeiten und Entwicklungen der Rumpfanregungspektroskopie mit zirkularpolarisierten Photonen *PhD Thesis* Hamburg
[17] Attenkofer K, Tröger L, Herrmann M and Brüggmann U 1998 *HASYLAB Annual Report* 1998
[18] Haubold H G *et al* 1989 *Rev. Sci. Instrum.* **60** 1943–6
[19] Goerigk G 2006 Electronic and computer upgrade at ASAXS Beamline JUSIFA *HASYLAB Annual Report* 2006
[20] Fuoss P H, Eisenberger P, Warburton W K and Bienenstock A 1981 *Phys. Rev. Lett.* **46** 1537–40
[21] Vainio U, Pirkkalainen K, Kisko K, Goerigk G, Kotelnikova N and Serimaa R 2007 *Eur. Phys. J.* D **42** 92–101
[22] Evans G and Pettifer R 2001 *J. Appl. Crystallogr.* **34** 82–6
[23] Evans G 2004 CHOOCH, Manual, Determination of Anomalous Scattering Factors from x-ray fluorescence data Q.3
[24] Kraft S, Stümpel J, Becker P and Kuetgens U 1996 *Rev. Sci. Instrum.* **67** 681–7
[25] Debye P, Anderson H J and Brumberger H 1957 *J. Appl. Phys.* **28** 679–83

[26] Goerigk G and Williamson D L 1998 *Solid State Commun.* **108** 419–24
[27] Goerigk G and Williamson D L 2001 *J. Non-Cryst. Solids* **281** 181–8
[28] Svergun D and Semenyuk A 2003 PROGRAM PACKAGE GNOM http://www.embl-hamburg.de/ExternalInfo/Research/Sax/
[29] Zhao Y, Feng Y, Cheng C, Zhou L, Wu Y, Machi T, Fudamoto Y, Koshizuka N and Murakam M 2001 *Appl. Phys. Lett.* **79** 1154
[30] Kramer M, Bud'ko S L, Canfield P, Wilke R, Finnemore D and Raymond J 2007 cond-mat. supr-con
Q.4 arXiv:condmat/0302443v1
[31] Wang Y, Wang H, Yang Y and Jiang Q 2008 *Mater. Sci. Eng.* A **478** 9–15
[32] Qiu D, Zhang M X, Fu H M, Kelly P and Taylor J 2007 *Phil. Mag. Lett.* **87** 505–14
[33] Singh S, Eijt S, Huot J, Kockelmann W, Wagemaker M and Mulder F 2007 *Acta Mater.* **55** 5549–57
[34] Dornheim M, Eigen N, Barkhordarian G, Klassen T and Bormann R 2006 *Adv. Eng. Mater.* **5** 377–85
[35] Zhou Y 2007 *Master's Thesis* Technical University of Hamburg-Harburg
[36] Lavrenko V, Vasil'ev A and Rokhlenko A 1974 *Theor. Exp. Chem.* **7** 564–7
[37] Samsonov G and Kharlamov A 1976 *Powder Metall. Met. Ceram.* **14** 699–707

## Queries for IOP paper 284535

*Journal:* **Nano**
*Author:* **U Bösenberg et al**
*Short title:* **Chemical state and distribution of additives in RHCs**

### Page 7

*Query 1:*
Author: Please check author name: Kharlamov given in reference.

### Page 8

*Query 2:-*
Author: [11]: Please check the journal title inserted.

*Query 3:-*
Author: [23]: Any more details?

### Page 9

*Query 4:-*
Author: [30]: Please check the pre-print number given.